

EHD Contact Modelling of Gleason Bevel Gears

Rolling-sliding machines such as gears, cams and followers, and bearings are often subjected to high loads, high speeds and high slip conditions, when not only the pressure distribution in the lubricant is a question but the surface deformation, and variation of the viscosity due to pressure, too. Although several methods have been already developed for solving elastohydrodynamic problems, the solution of the highly nonlinear problem is still quite challenging. So the development of a simulation method to determine the surface loading conditions is under special attention in order to be possible to calculate the sub-surface stress field. Gleason bevel gears have got a complex geometry which only can be described with the tools of differential geometry. In case of Gleason gear, solving of elastohydrodynamic problems is a great challenge for the engineers. The described elastohydrodynamic model takes into account the cavitation which is modelled by a special and own developed method. The problem was solved in finite element way using many supporting numerical methods. The developed p-version finite element model calculates the film shape and the pressure distribution. In this work, the lubricant film created on contacting piece of toroidal surface was defined by principal curvature of the global geometry of a given position of the moving Gleason gear. The calculation was successful, and as a result we got the film shape, the pressure field in the lubricant, the elastic deformation of the Gleason gear and the stress developed in the gear due to the contact.

Keywords: Gleason, bevel, gear, elastohydrodynamic, lubrication, cavitation, FEM.

Szabolcs Szávai

Head of Department
Bay Zoltán Nonprofit Ltd. for Applied
Research, Engineering Division (BAY-ENG)
Department of Structural Integrity
and Production Technologies, Miskolc
Hungary

Sándor Kovács

Postdoctoral Fellow
Bay Zoltán Nonprofit Ltd. for Applied
Research, Engineering Division (BAY-ENG)
Department of Structural Integrity
and Production Technologies, Miskolc
Hungary

1. INTRODUCTION

The generalized case of surface pairs contacting along a spot in the status of liquid friction is illustrated in Figure 1. The gap between the bodies is filled with lubricant due to the relative motion of the bodies and hydrodynamic pressure develops due to the movement of the lubricant. The movement of the lubricant is caused by the shear stress generated in the lubricant as the result of the relative motion of the surfaces. At the particular kinematic condition of the contacting bodies and with a given gap geometry, the pressure distribution acting on the surfaces is able to maintain balance with the force pressing the surfaces to each other and prevent a direct body-to-body contact thereby. For the contact problem of lubrication theory – due to its nature – it is convenient to employ in general a Descartes coordinate system with axis z perpendicular to the centre contact surface.

The film shape can be calculated as a superposition of the initial geometry, the displacement of a rigid surface and the deformation of a half-space under pressure. After deformation, the film shape is:

$$h = h_1 + h_2 = h_{g_1} + \Delta_{\text{rigid}_1} + \delta_1 + h_{g_2} + \Delta_{\text{rigid}_2} + \delta_2 = h_g + \Delta_{\text{rigid}} + \delta \quad (1)$$

where: h_g is the initial gap size, Δ_{rigid} is the relative rigid normal displacement between the contact bodies, and δ is the total deformation of the surfaces.

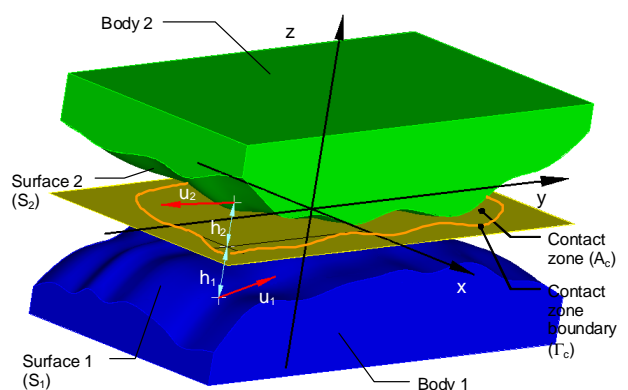


Figure 1. Contacting bodies

The classical approach to find the stresses and displacement in an elastic half-space due to surface traction was presented by Boussinesq (1885) and Cerruti (1882) and was developed by Love (1952). For this case, Johnson (1985) [1] reported a simple solution. Based on this, the deformation of the surface of the half-space under the action of a normal pressure in case of line contact is:

Received: April 2015, Accepted: July 2015

Correspondence to: Dr Szabolcs Szávai
Bay Zoltán Nonprofit Ltd. for Applied Research,
Iglói út 2, H-3519 Miskolc, Hungary
E-mail: szabolcs.szavai@bayzoltan.hu

doi:10.5937/fmet1503233S

$$\delta(x') = \frac{2}{\pi E'_s} \int p \ln(x' - x)^2 dx \quad (2)$$

where: E' is the equivalent Young modulus and s is the contact line.

The deformation due to thermal expansion is negligible in most cases. $\vec{u}_{xy}^T = [u_x, u_y]$: the velocity in the contact plane, u_z : the velocity in the z direction, $\nabla_{xy} = [\partial/\partial x, \partial/\partial y]$, W_i is the velocity of the contact bodies. Due to translation of the surfaces perpendicularly to the contact plane as:

$$u_z|_{z=-h_1} = W_1(t, x, y) - \vec{u}_{xy}|_{z=-h_1} (\nabla_{xy} h_1), \quad (3)$$

$$u_z|_{z=h_2} = W_2(t, x, y) + \vec{u}_{xy}|_{z=h_2} (\nabla_{xy} h_2). \quad (4)$$

The integral of the pressure over the contact area should be equal with the external load.

$$F_W = \int_{A_c} p dA \quad (5)$$

where: F_W is the normal load of the surfaces.

Loadcase can be satisfied if the Δ_{rigid} is a variable.

2. HYDRODYNAMIC PROBLEM INCLUDING CAVITATION

2.1 The generalized Reynolds equation

For calculating the contact pressure due to fluid film lubrication the generalized Reynolds equation was developed by Dowson (1961) [2] as a partial differential equation takes into account the changes of the viscosity and density across the film thickness.

$$\nabla_{xy} \bar{\Psi} - \nabla_{xy} (\nabla_{xy} p \Phi) - \Omega = 0 \quad (6)$$

where:

$$\Phi = F_2 + G_1, \quad (7)$$

$$\begin{aligned} \bar{\Psi} = & h_2 \rho_2 \vec{u}_{xy_2} - h_1 \rho_1 \vec{u}_{xy_1} - \\ & - \frac{(\vec{u}_{xy_2} - \vec{u}_{xy_1} - \vec{K}_{0,xy_2})}{F_0} (F_3 + G_2) - \\ & - \vec{u}_{xy_1} G_3 - \vec{K}_{1,xy} - \vec{K}_{2,xy}, \end{aligned} \quad (8)$$

$$\Omega = \rho_1 W_1 - \rho_2 W_2 - \int_{h_1}^{h_2} \frac{\partial \rho}{\partial t} dz. \quad (9)$$

The F_i , G_i and $\vec{K}_{i,xy}$ are viscosity-density functions:

$$F_0 = \int_{-h_1}^{h_2} \frac{F(\tau_{eq})}{\tau_{eq}} dz,$$

$$F_1 = \int_{-h_1}^{h_2} \frac{F(\tau_{eq})}{\tau_{eq}} z dz,$$

$$\begin{aligned} F_2 = & \int_{-h_1}^{h_2} \rho \frac{F(\tau_{eq})}{\tau_{eq}} z^2 dz - \frac{F_1 F_3}{F_0}, \\ F_3 = & \int_{-h_1}^{h_2} \rho \frac{F(\tau_{eq})}{\tau_{eq}} z dz, \end{aligned} \quad (10)$$

$$\begin{aligned} G_1 = & \int_{-h_1}^{h_2} z \frac{\partial \rho}{\partial z} \left(\int_{-h_1}^z \frac{F(\tau_{eq})}{\tau_{eq}} \bar{z} dz - \frac{F_1}{F_0} \int_{-h_1}^z \frac{F(\tau_{eq})}{\tau_{eq}} d\bar{z} \right) dz, \\ G_2 = & \int_{-h_1}^{h_2} z \frac{\partial \rho}{\partial z} \left(\int_{-h_1}^z \frac{F(\tau_{eq})}{\tau_{eq}} d\bar{z} \right) dz, \\ G_3 = & \int_{-h_1}^{h_2} z \frac{\partial \rho}{\partial z} dz, \end{aligned} \quad (11)$$

$$\vec{K}_{0,xy} = \int_{-h_1}^{h_2} A \frac{d\vec{\sigma}'_z}{dt} dz = \begin{bmatrix} \int_{-h_1}^{h_2} \frac{Ad\tau_{xz}}{dt} dz \\ \int_{-h_1}^{h_2} \frac{Ad\tau_{yz}}{dt} dz \end{bmatrix},$$

$$\vec{K}_{1,xy} = \int_{-h_1}^{h_2} z \rho A \frac{d\vec{\sigma}'_z}{dt} dz,$$

$$\vec{K}_{2,xy} = \int_{-h_1}^{h_2} z \frac{\partial \rho}{\partial z} \left(\int_{-h_1}^z A \frac{d\vec{\sigma}'_z}{dt} d\bar{z} \right) dz, \quad (12)$$

where: $F(\tau_{eq})$ is a function characteristic of a particular lubricant model, while τ_{eq} is the equivalent shear stress.

The function $F(\tau_{eq})$ in (10) and (11) may take the following forms, for example in the case of various types of lubricant models on the basis of [3]:

$$F(\tau_{eq})_{\text{Newton}} = \frac{\tau_{eq}}{\eta},$$

$$F(\tau_{eq})_{\text{Eyring}} = \frac{\tau_E}{\eta} \sinh\left(\frac{\tau_{eq}}{\tau_E}\right),$$

$$F(\tau_{eq})_{\text{viscoplastic}} = -\frac{\tau_L}{\eta} \ln\left(1 - \frac{\tau_{eq}}{\tau_L}\right),$$

$$F(\tau_{eq})_{\text{simple viscoplastic}} = -\frac{\tau_{eq}}{\eta} \left(1 - \left|\frac{\tau_{eq}}{\tau_L}\right|\right)^{-1},$$

$$F(\tau_{eq})_{\text{circular}} = \frac{\tau_{eq}}{\eta} \left[1 - \left(\frac{\tau_{eq}}{\tau_L}\right)^2\right]^{-1/2}, \quad (13)$$

where: τ_E is the Eyring shear stress, while τ_L is the limit shear stress.

The τ_L can be considered linearly proportional to pressure and described with parameters τ_{l0} and χ as:

$$\tau_L = \tau_{l0} + \chi p. \quad (14)$$

2.2 Transformation z coordinate to dimensionless ζ

Since the problem is independent from the contact plane position, the coordinate system can be attached to the bottom surface as it is usually done. Furthermore, let us introduce the dimensionless coordinate ζ along the gap as defined in (15) and (16) and let the coordinate z be the linear function of ζ :

$$\begin{aligned} z|_{S_q} &= -h_1 = 0 & \zeta &= -1, \\ z|_{S_q} &= h_2 = h & \zeta &= 1, \end{aligned} \quad (15)$$

$$z = h \left(\frac{1 + \zeta}{2} \right). \quad (16)$$

Applying the z - ζ coordinate transformation, the integration across the thickness becomes independent of the gap size.

$$\begin{aligned} F_0 &= \frac{h}{2} \int_{-1}^1 \frac{F(\tau_{eq})}{\tau_{eq}} d\zeta = \frac{h}{2} f_0, \\ F_1 &= \frac{h^2}{2} \int_{-1}^1 \frac{F(\tau_{eq})}{\tau_{eq}} \left(\frac{1 + \zeta}{2} \right) d\zeta = \frac{h^2}{2} f_1, \\ F_2 &= \frac{h^3}{2} \left(\int_{-1}^1 \rho \frac{F(\tau_{eq})}{\tau_{eq}} \left(\frac{1 + \zeta}{2} \right)^2 d\zeta - \frac{f_1 f_3}{f_0} \right) = \frac{h^3}{2} f_2, \\ F_3 &= \frac{h^2}{2} \int_{-1}^1 \rho \frac{F(\tau_{eq})}{\tau_{eq}} \left(\frac{1 + \zeta}{2} \right) d\zeta = \frac{h^2}{2} f_3, \end{aligned} \quad (17)$$

$$\begin{aligned} G_1 &= \frac{h^3}{2} \int_{-1}^1 \frac{\partial \rho}{\partial \zeta} \left(\frac{1 + \zeta}{2} \right) \left(\int_{-1}^{\zeta} \frac{F(\tau_{eq})}{\tau_{eq}} \left(\frac{1 + \bar{\zeta}}{2} \right) d\bar{\zeta} - \right. \\ &\quad \left. - \frac{f_1}{f_0} \int_{-1}^{\zeta} \frac{F(\tau_{eq})}{\tau_{eq}} d\bar{\zeta} \right) d\zeta = \frac{h^3}{2} g_1, \\ G_2 &= \frac{h^2}{2} \int_{-1}^1 \left(\frac{1 + \zeta}{2} \right) \frac{\partial \rho}{\partial \zeta} \left(\int_{-1}^{\zeta} \frac{F(\tau_{eq})}{\tau_{eq}} d\bar{\zeta} \right) d\zeta = \frac{h^2}{2} g_2 \\ G_3 &= h \int_{-1}^1 \left(\frac{1 + \zeta}{2} \right) \frac{\partial \rho}{\partial \zeta} d\zeta = h g_3, \end{aligned} \quad (18)$$

$$\int_0^h \frac{\partial \rho}{\partial t} dz = \frac{h}{2} \int_{-1}^1 \frac{\partial \rho}{\partial t} d\zeta, \quad (19)$$

$$\begin{aligned} \bar{K}_{0,xy} &= \frac{h}{2} \int_{-1}^1 A \frac{d\bar{\sigma}'_z}{dt} d\zeta = \frac{h}{2} \bar{k}_{0,xy}, \\ \bar{K}_{1,xy} &= \frac{h^2}{2} \int_{-1}^1 \left(\frac{1 + \zeta}{2} \right) \rho A \frac{d\bar{\sigma}'_z}{dt} d\zeta = \frac{h^2}{2} \bar{k}_{1,xy}, \\ \bar{K}_{2,xy} &= \frac{h^2}{2} \int_{-1}^1 \left(\frac{1 + \zeta}{2} \right) \frac{\partial \rho}{\partial \zeta} \left(\int_{-1}^{\zeta} A \frac{d\bar{\sigma}'_z}{dt} d\bar{\zeta} \right) d\zeta = \\ &= \frac{h^2}{2} \bar{k}_{2,xy}. \end{aligned} \quad (20)$$

Since the h can be handled separately from the integration as an independent variable the problem can be reduced to a quasi 2D case based on the hydrodynamic lubrication theory developed by Reynolds. Furthermore, special lubricant film element can be developed for finite-element modelling of such problems.

2.3 Penalty cavitation

Nevertheless, the generalized Reynolds equation is not valid for the region where cavitation can occur and the lubricant is stuck onto the surface and is flowing in stripes. For extending the governing equation to the cavitation zone the Elrod-Adams algorithm is the most well-known one that introduces the $\theta = \rho/\rho_c$ fractional film content [4]. However, Elrod algorithm has some disadvantages due to the discrete values (0, 1) of the cavitation index, which can occasionally cause oscillation. A method for FEM solution has been published by Kumar and Booker [5,6]. The method separates the pressure calculation in the contact zone from the density determination. Kumar and Booker also proposed to use linear correlation between the density and the viscosity in the cavitation zone as follows:

$$\frac{\eta}{\eta_L} = \frac{\rho}{\rho_L}; \quad \rho \leq \rho_c. \quad (21)$$

Instead of the separation of the variables for the contact and cavitation zone, penalty cavitation method has been proposed by Szávai [7], where the density change as a function of the pressure in the cavitation zone let to be approximated by a high gradient slope under the cavitation pressure. The above described criteria can be satisfied with the following density function:

$$\rho^* = \frac{\rho_L(p, \vartheta)}{\gamma(p)(p_c - p) + 1} \quad (22)$$

where: $\gamma(p)$ is the penalty function which is 0 if $p > p_c$ otherwise $\gamma(p) = c$, where c is a sufficiently high number.

It has to be noticed that the density depends on the pressure not only in the lubrication region, but in the cavitation zone as well. The ρ^* is valid in the lubrication region and the cavitation zone as well, and the volume fraction can be written as:

$$\theta(p) = \frac{\rho^*}{\rho_L} = \frac{1}{\gamma(p)(p_c - p) + 1}. \quad (23)$$

Applying the linear correlation between the density and the viscosity according to Kumar and Booker the viscosity can be written as follows:

$$\eta^* = \eta_L(p, \vartheta) \frac{\rho^*}{\rho_L(p, \vartheta)} = \theta(p) \eta_L(p, \vartheta). \quad (24)$$

2.4 The modified generalized Reynolds equation

Based on the concepts above the generalized Reynolds equation with penalty cavitation extension is:

$$R(p, \rho, \dot{\rho}, h, t, \eta, \bar{u}_1, \dots) = \nabla_{xy} \left(\theta h \bar{\psi} + \theta \frac{h^2}{2} \bar{k}_{xy} \right) - \nabla_{xy} \left(\frac{h^3}{2} \phi \nabla_{xy} p \right) - \theta \left(\rho_1 W_1 - \rho_2 W_2 - \frac{h}{2} \omega_{dt} \right) = 0 \quad (25)$$

while the mass-flow in the gap is:

$$\bar{q}_h = \theta \left(h \bar{\psi} + \frac{h^2}{2} \bar{k}_{xy} \right) - \frac{h^3}{2} \phi \nabla_{xy} p \quad (26)$$

where: w is a weight function.

$$\phi = f_2 + g_1, \quad (27)$$

$$\bar{\psi} = \rho_2 \bar{u}_{xy_2} - \frac{(\bar{u}_{xy_2} - \bar{u}_{xy_1})}{f_0} (f_3 + g_2) - \bar{u}_{xy_1} g_3, \quad (28)$$

$$\bar{k}_{xy} = \frac{f_3 + g_2}{f_0} \bar{k}_{0xy} - \bar{k}_{1xy} - \bar{k}_{2xy}, \quad (29)$$

$$\omega_{dt} = \int_{-1}^1 \frac{\partial \rho}{\partial t} d\chi + \frac{\partial}{\partial t} \ln \theta(p) \int_{-1}^1 \rho d\chi. \quad (30)$$

In equation (25) both variables h and p can be seen clearly, furthermore $\bar{\psi}$, \bar{k}_{xy} , ω_{dt} are nonlinear functions of the lubricant material properties only and it can be used for determination of both variables depending on whether a direct or an inverse solution technique is chosen.

3. FINITE ELEMENT DISCRETIZATION

For the discretized governing equations, the weak form of the weighted-residual integral form of the Reynolds equation has been applied. Legendre or Lagrange functions [8] have been used for the polynomial approximation of the unknown pressure and surface deformation.

In the case of variation methods, the integral forms of the differential equations are used and in the course of this, rationally, certain quantities have to be integrated over the region investigated. The integration range has to be divided into shapes characteristic of a particular element type for the use of the finite element method and then derived into a unified shape by means of conform transformation for numerical integration.

The edges and sides of the elements along the gap are parallel with coordinate axis z and thus the unit vector \mathbf{e}_z of the global coordinate system connected to the contact surface and unit vector \mathbf{e}_z of the coordinate system connected to the element coincide. Consequently, x and y coordinates, the gap size and the pressure are not the functions of ζ :

$$x^e(\xi, \eta, t) = \sum_i X_i^e(t) N_{xi}^e(\xi, \eta) = \mathbf{N}_x^{eT}(\xi, \eta) \mathbf{X}^e(t) \quad (31)$$

$$y^e(\xi, \eta, t) = \sum_j Y_j^e(t) N_{yj}^e(\xi, \eta) = \mathbf{N}_y^{eT}(\xi, \eta) \mathbf{Y}^e(t) \quad (32)$$

$$h_g^e(\xi, \eta, t) = \sum_j H_{gj}^e(t) N_{hj}^e(\xi, \eta) = \mathbf{N}_g^{eT}(\xi, \eta) \mathbf{H}_g^e(t) \quad (33)$$

$$\delta_i^e(\xi, \eta, t) = \sum_j H_{\delta_j}^e(t) N_{\delta_j}^e(\xi, \eta) = \mathbf{N}_g^{eT}(\xi, \eta) \mathbf{H}_{\delta_i}^e(t); \quad i=1,2 \quad (34)$$

$$h^e = \left[\mathbf{N}_g^{eT}, 1 \right] \begin{bmatrix} \mathbf{H}_g^e + \mathbf{H}_{\delta_1}^e + \mathbf{H}_{\delta_2}^e \\ \Delta_{\text{rigid}} \end{bmatrix} = \mathbf{N}_h^{eT}(\xi, \eta) \mathbf{H}^e(t) \quad (35)$$

$$p^e(\xi, \eta, t) = \sum_j P_j^e(t) N_{pj}^e(\xi, \eta) = \mathbf{N}_p^{eT}(\xi, \eta) \mathbf{P}^e(t). \quad (36)$$

The approximation of coordinate z is necessary if the thermodynamical problem or non-Newtonian lubricant is also taken into consideration. Since z is linear in ζ :

$$z^e = h^e \left(\frac{1+\zeta}{2} \right) = \left(\frac{1+\zeta}{2} \right) \mathbf{N}_h^{eT} \mathbf{H}^e. \quad (37)$$

A primary task in the application of variation principles is to determine which field should be determined from which equation by its variation. In the present case, the purpose is to determine 5 unknown fields: pressure p , displacements δ_{pi} ($i = 1, 2$) caused by the pressures of the two surfaces as well as the displacements Δ_{rigid} , of the bodies like rigid bodies.

3.1 The weak integral form of the Reynolds equation

Based on the concepts of it, the weak integral form of the generalized Reynolds equation is:

$$\int_{A_c} \nabla_{xy} w_R \left(\theta \left(h \bar{\psi} + \frac{h^2}{2} \bar{k}_{xy} \right) - \frac{h^3}{2} \phi \nabla_{xy} p \right) - w_R \theta \Omega_\gamma dA - \oint_{\Gamma_c} w_R q_h^{n\Gamma} d\Gamma = 0. \quad (38)$$

For the discretized governing equations, the weak form of the weighted-residual integral form of the Reynolds equation has been applied. The popularity of the solutions based on the weak integral form is understandable since it is advantageous in the course of solving hydrodynamic problems that it imposes less severe requirements in respect of continuity and thus contains only differentials of the first degree in respect of pressure and gap size.

Let the weight functions be $w_R = \mathbf{N}_R$, furthermore applying the approximation (34) and (35) of the pressure and gap size, the discretized equation (39) is obtained instead of (38):

$$\mathbf{R} = \int_{A_c} \phi \frac{h^3}{2} \mathbf{B}_R^T \mathbf{B}_p dA \mathbf{P} - \int_{A_c} \theta \mathbf{B}_R^T \psi \mathbf{N}_h^T dA \mathbf{H} - \int_{A_c} \theta \mathbf{B}_R^T \frac{h}{2} \mathbf{k}_{xy} \mathbf{N}_h^T dA \mathbf{H} - \int_{A_c} \theta \Omega_\gamma \mathbf{N}_R dA - \oint_{\Gamma_c} q_h^{n\Gamma} \mathbf{N}_R d\Gamma = \mathbf{0} \quad (39)$$

where: $\nabla_{xy} \mathbf{N}_p^T = \mathbf{B}_p$ and $\nabla_{xy} \mathbf{N}_R^T = \mathbf{B}_R$.

The discretized Reynolds equation takes the following form as the result:

$$\begin{aligned} \mathbf{R} &= \mathbf{R}(\mathbf{P}, \rho, \dot{\rho}, h, \bar{r}, t, \eta, \tau_{\text{eq}}, \vartheta, \theta, \bar{u}_1, \bar{u}_2, \dots) = \\ &= \mathbf{S}_\phi \mathbf{P} - \mathbf{S}_\psi \mathbf{H} - \mathbf{S}_k \mathbf{H} - \mathbf{R}_\Omega - \mathbf{R}_q = \mathbf{0}. \end{aligned} \quad (40)$$

The equation (40) contains the discretized pressure and gap size. The w_R weight functions are $\mathbf{N}_R = \mathbf{N}_p$ in case of direct solution. If inverse solution is chosen the w_R weight function should be $\mathbf{N}_R = \mathbf{N}_g$.

The pressure and deformation fields are connected by the linear or nonlinear solid mechanical description of the surfaces. Furthermore, the pressure distribution has to satisfy the load case in (5).

3.2 Discretized deformation

In respect of this discussion of the problem of elastohydrodynamic lubrication the mode of determining the deformations is not a central issue. It is sufficient to presume that the change in gap size $\delta_i(p, x, y)$ is a mutually continuous function of the pressure distribution. Functions $\delta_i(p, x, y)$ may be determined by numerical and analytical methods alike. Let us assume for the solution of this set of problems that the equations that follow are in existence:

$$L_{pi}(p(x, y), \delta_{pi}(x, y)) = 0. \quad (41)$$

The calculation of displacements occurring under the effect of the distributed load acting on the surface is already a routine task in the range of numerical methods by now and thus the equations needed for this will not be detailed either. In respect of this problem it is sufficient to accept that after introducing approximations (33) and (35), equation (40) will take the following form of the set of algebraic equations if the displacement is presumed to be quasi-static. The finite element equilibrium equation associated with the displacement due to pressure is:

$$\mathbf{K}_{pi}(\delta_{pi}) \mathbf{H}_{\delta_{pi}} + \mathbf{f}_{pi}(p) = \mathbf{0}. \quad (42)$$

The reduced nodal loading vectors associated with pressure p are:

$$\mathbf{f}_{pi}(p) = \mathbf{C}_{pi}(\mathbf{P}) \mathbf{P}. \quad (43)$$

If analytical solution is used for the deformation calculation as it is shown in equation (2), the equation (41) will be:

$$\begin{aligned} &\int_{s_c} \mathbf{N}_h \mathbf{N}_h^T dA \mathbf{H}_{\delta_{pi}} - \frac{2}{\pi E_i} \cdot \\ &\cdot \int_{s_c} \mathbf{N}_h \int_{A_c} \ln(x' - x)^2 \mathbf{N}_p^T ds(\hat{x}) ds(x) \mathbf{P} = 0. \end{aligned} \quad (44)$$

On this basis for direct solution the deformation matrix may also be written in respect of the displacements due to the pressure distribution for direct or inverse solution as:

$$\mathbf{H}_{\delta_{pi}} = \mathbf{K}_{pi}^{-1} \mathbf{C}_{pi} \mathbf{P} = \mathbf{D}_{pi} \mathbf{P}, \quad (45)$$

$$\mathbf{P} = \mathbf{K}_p \mathbf{C}_p^{-1} \mathbf{H}_{\delta_p} = \mathbf{D}_p^{-1} \mathbf{H}_{\delta_p}. \quad (46)$$

3.3 Linearization of the equations for EHD problem

The difficulty of reaching a solution in the subject matter investigated is caused primarily by the strongly nonlinear nature of the Reynolds equation. The solutions of strongly nonlinear equations are based in the vast majority of cases on the Newtonian or gradient methods.

Consequently, the discretized Reynolds equation system has to be linearized in order to enable the determination of the pressure distribution and the associated gap size. Let us observe the equation as:

$$\mathbf{R} = \mathbf{R}(\mathbf{P}, \rho, \dot{\rho}, h, \bar{r}, t, \eta, \tau_{\text{eq}}, \vartheta, \theta, \bar{u}_1, \bar{u}_2, \dots). \quad (47)$$

The linearized form of this at an arbitrary point $\mathbf{H} = \mathbf{H}^j$, $\mathbf{P} = \mathbf{P}^j$ is:

$$\begin{aligned} &{}^i \mathbf{R}(\mathbf{H}^j, \mathbf{P}^j, {}^{i-1} \mathbf{R}) + \\ &+ \left(\frac{\partial^i \mathbf{R}}{\partial \mathbf{P}} + \frac{\partial^i \mathbf{R}}{\partial \rho} \frac{\partial \rho}{\partial p} \mathbf{N}_p + \frac{\partial^i \mathbf{R}}{\partial \eta} \frac{\partial \eta}{\partial p} \mathbf{N}_p \right) \Bigg|_{\mathbf{H}^j, \mathbf{P}^j} \Delta \mathbf{P} + \\ &+ \left(\frac{\partial^i \mathbf{R}}{\partial \mathbf{H}} + \frac{\partial^i \mathbf{R}}{\partial h} \mathbf{N}_h \right) \Bigg|_{\mathbf{H}^j, \mathbf{P}^j} \Delta \mathbf{H} + O = \mathbf{0}. \end{aligned} \quad (48)$$

The equation for the deformation also has to be linearized as follows for direct or inverse solution:

$$\mathbf{H}_{\delta_i}^j - \mathbf{D}_i \Big|_{\mathbf{H}_{\delta_i}^j, \mathbf{P}^j} \mathbf{P}^j + \Delta \mathbf{H}_{\delta_i}^j - \mathbf{D}_i \Big|_{\mathbf{H}_{\delta_i}^j, \mathbf{P}^j} \Delta \mathbf{P} = \mathbf{0}, \quad (49)$$

$$\mathbf{D}_i^{-1} \Big|_{\mathbf{H}_{\delta_i}^j, \mathbf{P}^j} \mathbf{H}_{\delta_i}^j - \mathbf{P}^j + \mathbf{D}_i^{-1} \Big|_{\mathbf{H}_{\delta_i}^j, \mathbf{P}^j} \Delta \mathbf{H}_{\delta_i}^j - \Delta \mathbf{P} = \mathbf{0}. \quad (50)$$

The load case in linearized form is:

$$F_W - \int_{A_c} \mathbf{N}_p dA \mathbf{P}^j - \int_{A_c} \mathbf{N}_p dA \Delta \mathbf{P} = 0. \quad (51)$$

4. APPLICATION FOR THE GLEASON BEVEL GEARS

4.1 Numerical solution of the system of equations

The EHD was solved in iteration loop. In this case, the Newton-Raphson method has been used. Due to the strongly nonlinearity, the solutions have to be stabilized.

Complex step optimization was required for the EHD problem. The solution of the EHD problem would be ${}^i \mathbf{P}^*$ where the residual ${}^i \mathbf{R} = 0$. Let ${}^i \mathbf{P}^*$ be approximated with a series of solutions for $\Delta \mathbf{P}^j$ in this equation as shown:

$$\mathbf{P}^{j+1} = \mathbf{P}^j + \alpha \Delta \mathbf{P}^j; \quad \alpha = [0 \dots 1]. \quad (52)$$

As the initial system of equations is highly nonlinear in the case of EHD problems, it is very difficult to find an initial state where the instability of the solution can be avoided. For this reason, a properly chosen α is required.

Experience has shown that $\alpha < 0.1$ was satisfactory.

4.2 Solution of the elastohydrodynamic problem of the Gleason bevel gears

We will demonstrate the suitability of the method developed in the next example.

In contrast to the contact surfaces of simpler and constant geometry, the case of the Gleason bevel gear is much more complex. The contact geometry of the gap changes during operation from point to point with the rotation of the gear.

Also, the contact area migrates on a complex surface which can be described only with differential geometry tools. Surface geometry belonging to each position can be described only by principal curvatures and principal curvature directions. The velocity of the contacting surface changes from point to point with the migration of the contact area.

In this example, we solved the elastohydrodynamic problem belonging to contact area of a given position of the Gleason bevel gears.

In this case we had a conical pinion gear with concave-sided flank, 9 teeth, right tooth bending contacts with crown gear with convex-sided flank, 33 teeth, left tooth bending.

The problem was isothermal so the density and the viscosity are constant along the thickness. Thus the G_1 , G_2 , G_3 coefficients are zero.

The EHD problem was stationary, so the time derivatives were zero.

Load is $F = 1750$ N.

Newtonian lubricant was chosen, which causes that K_{0xy} , K_{1xy} , K_{2xy} are zero. The viscosity of the lubricant was given by the Barus equation:

$$\eta = \eta_0 e^{\frac{\alpha p}{E}}, \quad (53)$$

where: $\alpha = 5000$, $\eta_0 = 0.01539$ Pas.

The Young modulus of the solid body of the gears is $E = 219.8$ GPa, and the Poisson ratio $\nu = 0.3$.

The main extents of the ellipse of the contact area in the given position are:

- Major semiaxis: $a = 4.015$ mm.
- Minor semiaxis: $b = 0.321$ mm.

The principal curvatures and directions of the principal curvatures defining the contacting solid surfaces are the following.

Principal curvatures:

- Crown gear with convex-sided flank: $k_{12} = 0$ mm⁻¹; $k_{112} = 6.2359 \times 10^{-3}$ mm⁻¹.
- Conical pinion gear with concave-sided flank: $k_{11} = 0.03423$ mm⁻¹; $k_{111} = 6.2359 \times 10^{-3}$ mm⁻¹.

Directions of the principal directions form an angle. The direction of k_{11} and k_{12} form a 16.68 degree angle. Naturally, it is also true for the k_{111} and k_{112} .

The revolution of the conical pinion gear is 300 min⁻¹.

The velocity vectors of the lower and upper surface in the contact point after the linear transforming the contact plane to the X - Y plane [mm/s]:

$$\mathbf{v}_1 = \begin{bmatrix} 669.6 \\ 29.84 \\ 0 \end{bmatrix}; \quad \mathbf{v}_2 = \begin{bmatrix} 367.47 \\ 226.65 \\ 0 \end{bmatrix}. \quad (54)$$

The numerical results of the specific configuration can be seen in Figures 2 to 9. In Figure 2 it can be seen the pressure peak in the lubrication of which contact area is angular with the y -axis, so it takes up a general position. Thus the symmetry planes cannot be used for the simpler modelling. In Figure 3 it can be seen that next to the pressure peak zone the cavitation zone with negative pressure is displayed.

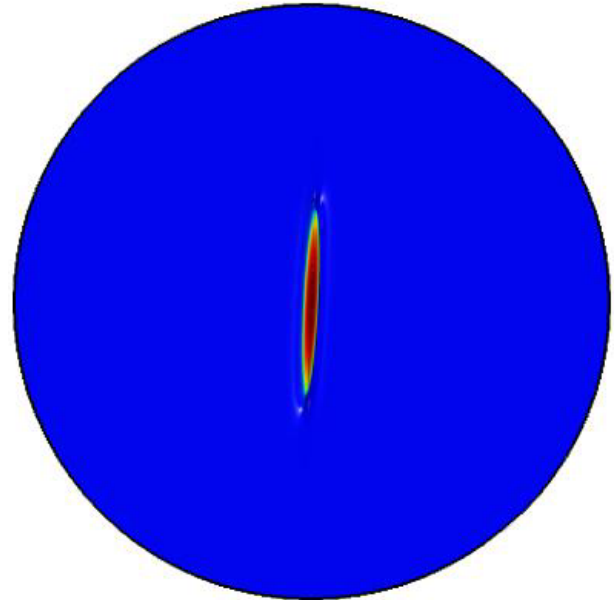


Figure 2. Awakening lubricant pressure field of the contact zone, top view

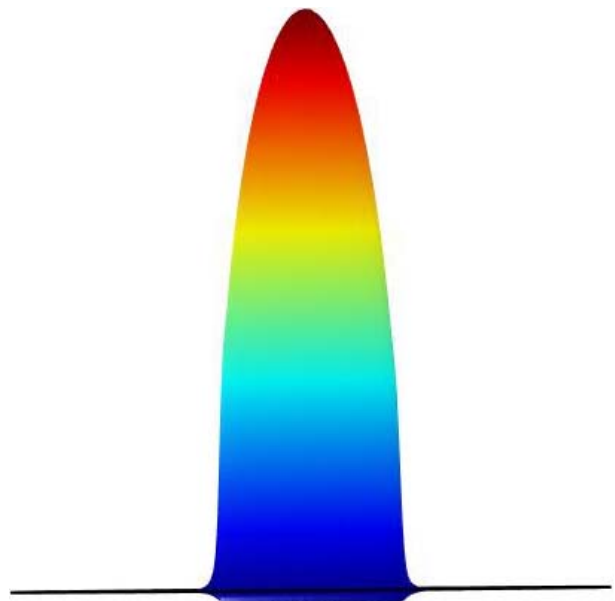


Figure 3. Awakening lubricant pressure field of the contact zone, side view

The stress maximum in the solid body of the gear is reached under the surface in significant depth, as illustrated in Figure 4. The deformation of the gear surface as results from the pressure field of the hydrodynamic lubrication can be seen in Figure 5.

In Figures 6 and 7 it can be seen the pressure field and gap thickness in the direction corresponds to the x axis. In Figures 8 and 9 it can be seen the pressure field and gap thickness in the direction corresponding to the y axis.

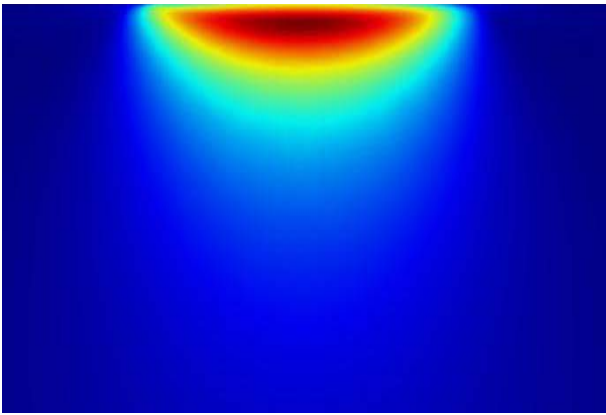


Figure 4. Awakening Mises stress distribution in the solid body under the contact zone, sectional drawing



Figure 5. Elastic deformation on the surface of the gears, top view

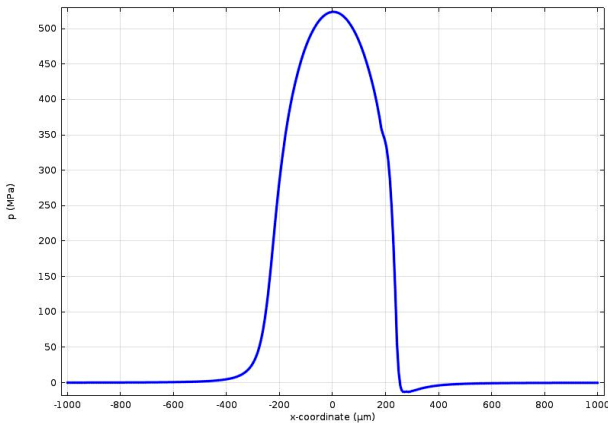


Figure 6. The pressure field awakening in lubrication, along the x axis

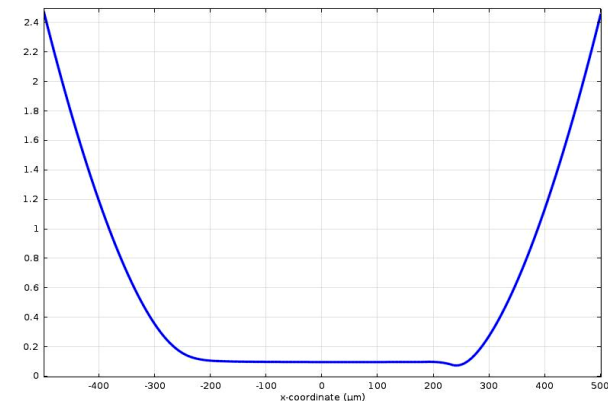


Figure 7. The gap thickness at the contact of the Gleason gears, along the x axis

In both Figures 6 and 8 it can be seen pressures increase next to the cavitation zone. These pressure accures will increase significantly due to the external load increasing, and stressed strongly the solid part of the gear below them, which can lead to failure.

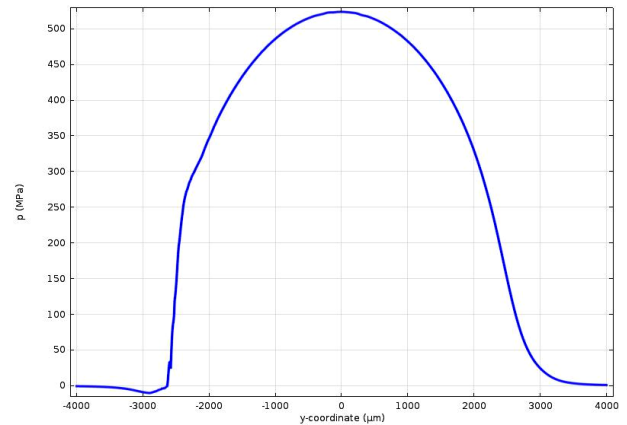


Figure 8. The pressure field awakening in lubrication, along the y axis

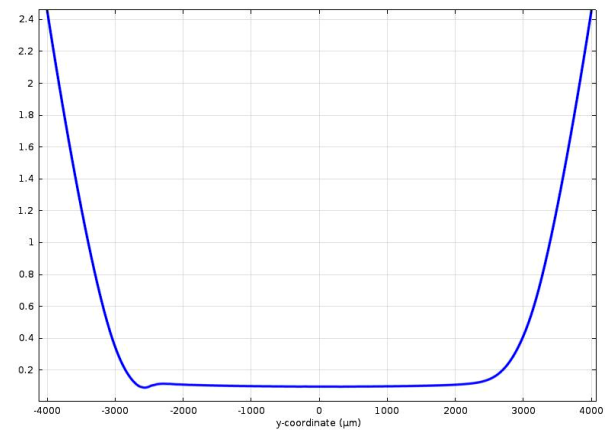


Figure 9. The gap thickness at the contact of the Gleason gears, along the y axis

5. CONCLUSION

Summarising the results of the calculations, we can state that the p-FEM method is a good and stable process to solve the EHD lubrication problems. A penalty parameter method for viscosity is applicable for the advanced numerical methods, such as for the p-version finite element method. Integration through the thickness is carried out by making use of dimensionless thickness coordinate. Furthermore, pressure and film thickness can be handled as independent element variables. Further effort will be done for testing the inverse solution possibility and for extending the model to spot contact as well.

So the development of a simulation method to determine the surface loading conditions is under special attention in order to be possible to calculate the sub-surface stress field.

ACKNOWLEDGMENT

The research work presented in this paper was carried out as part of the TÁMOP-4.2.2.A-11/1/KONV-2012-0036 project in the framework of the New Széchenyi Plan. The realization of this project is supported by the European Union, and co-financed by the European Social Fund.

REFERENCES

- [1] Johnson, K.L.: *Contact Mechanics*, Cambridge University Press, Cambridge, 1987.
- [2] Dowson, D.: A generalized Reynolds equation for fluid-film lubrication, *International Journal of Mechanical Sciences*, Vol. 4, No. 2, pp. 159-170, 1962.
- [3] Szeri, A.Z.: *Fluid Film Lubrication: Theory and Design*, Cambridge University Press, Cambridge, 1998.
- [4] Elrod, H.G.: A cavitation algorithm, *Transactions of the ASME, Journal of Lubrication Technology*, Vol. 103, No. 3, pp. 350-354, 1981.
- [5] Kumar, A. and Booker, J.F.: A finite element cavitation algorithm: Application/validation, *Transactions of the ASME, Journal of Tribology*, Vol. 113, No. 2, pp. 255-260, 1991.
- [6] Kumar, A. and Booker, J.F.: A finite element cavitation algorithm, *Transactions of the ASME, Journal of Tribology*, Vol. 113, No. 2, pp. 276-284, 1991.
- [7] Szávai, Sz.: Efficient p-version FEM solution for TEHD problems with new penalty-parameter based cavitation model, in: *Proceedings of the International Conference BALTRIB'2009*, 19-21.11.2009, Kaunas (Lithuania), pp. 239-245.
- [8] Páczelt, I.: *Finite Element Method in Engineering Practice I. Part*, Miskolci Egyetemi Kiadó, Miskolc, 1999, (in Hungarian).

МОДЕЛИРАЊЕ КОНТАКТА ИЗМЕЂУ КОНУСНИХ ЗУПЧАНИКА КОМПАНИЈЕ „ГЛЕЈСОН“ ПРИ ЕХД ПОДМАЗИВАЊУ

Саболч Саваи, Шандор Ковач

Машински елементи као што су зупчasti преносници, брегasti механизми и котрљајни лежаји често раде у условима котрљања са високим степеном клизањем и при великим специфичним оптерећења и брзинама. У тим случајевима, на расподелу притиска у слоју мазива утичу и деформације контактних површина, као и промена вискозности мазива услед промене притиска у слоју мазива. До сада је развијено неколико метода за добијање радних параметара при еластохидродинамичком подмазивању (ЕХДП) за једноставније геометрије, али је добијање тих параметара за комплексне геометрије још увек проблематично. Посебно је занимљиво развијање методе симулације услова рада којом се добија оптерећење контактне површине, како би на основу тога било могуће да се израчуна расподела напона испод саме површине. Конусни зупчаници компаније *Глејсон* имају комплексну геометрију која може да се опише једино помоћу техника диференцијалне геометрије. Добијање параметара ЕХДП код ових зупчастих парова је и даље изазов за инжењере. У раду је описан модел ЕХДП који узима у обзир појаву кавитације у мазиву. Овај модел је добијен коришћењем специјалне методологије развијене од стране аутора. Решење је добијено коришћењем методе коначних елемената и разних помоћних нумеричких метода. На основу разрађене „р“ верзије модела са коначним елементима су израчунати облик слоја мазива и расподела притиска у њему. Разматран је слој мазива у одређеном тренутку, формиран између контактних тороидалних површина које су дефинисане преко геометрије зупчаника. Прорачун се показао успешним и као резултат су добијени облик слоја мазива, расподела притиска у слоју мазива, еластична деформација зупчаника и напонско стање у зупчанику.